A theory of magnetic x-ray diffraction enhanced by an electric quadrupole (E2) resonance

1998 J. Phys.: Condens. Matter 10 501

(http://iopscience.iop.org/0953-8984/10/2/028)

J. Phys.: Condens. Matter **10** (1998) 501–524. Printed in the UK PII: S0953-8984(98)87340-2

A theory of magnetic x-ray diffraction enhanced by an electric quadrupole (E2) resonance

Stephen W Lovesey†, Oliver Fritz†§ and Ewald Balcar‡

† ISIS Facility, Rutherford Appleton Laboratory, Oxfordshire OX11 0QX, UK

‡ Atominstitut der Österreichischen Universitäten, A-1020 Vienna, Austria

Received 4 September 1997, in final form 27 October 1997

Abstract. The electric quadrupole contribution to the scattering length is derived using an atomic model for the resonant ion. At one of the levels of approximation considered, our so-called idealized scattering length is totally consistent with the standard sum rules for the analysis of the attenuation coefficient. A superior estimate of the scattering length includes the structure of the core state.

The two levels of treatment are used to discuss the intensity of x-rays Bragg diffracted by resonant lanthanide ions in a crystal. Using a ground state for the valence shell specified by Hund's rules, explicit expressions for the idealized scattering length are tabulated for the tripositive ions.

The general expressions for the scattering length can be evaluated for a valence-shell wave function of an arbitrary complexity. Thus, our scattering lengths can accommodate the influence of a crystal-field potential or a full multiplet calculation.

Linear and circular polarization in the primary and secondary beams of x-rays are handled in terms of a Stokes vector, and several illustrative calculations are given.

1. Introduction

Resonance enhancement of the magnetic diffraction of x-rays seems to have been first reported by Namikawa *et al* (1985), in a paper on x-ray scattering from ferromagnetic nickel at an energy very close to the K-shell absorption edge. Later, and inspired by observations reported by Gibbs *et al* (1988), Hannon *et al* (1988) argued that the enhancement is due to electric multipole absorption events. Their selection rules for the polarization dependence of the diffracted signal have been confirmed in a number of experiments on a variety of magnetic materials; for references to the experimental studies see, for example, Hill and McMorrow (1996) and Lovesey and Collins (1996).

At an energy well above the absorption edges, the amplitude for magnetic diffraction is very small compared to the amplitude for charge diffraction. Hence, resonance enhancement of the magnetic amplitude, typically by an order of magnitude or more, is a significant and most welcome help in using x-ray Bragg diffraction to study the properties of unpaired electrons in crystalline materials.

Materials that contain lanthanide ions are good candidates for such studies, and their magnetic properties are both intriguing and of great interest for some applications. At the L_2 and L_3 absorption edges of the ions the observed enhancements of the diffraction signal are very healthy. In consequence, magnetic signals can be measured with a good accuracy

§ On leave from the Paul Scherrer Institut, Switzerland.

0953-8984/98/020501+24$19.50

relatively quickly, particularly when the Bragg position is nominally purely magnetic in its character, e.g. a magnetic satellite reflection from a spiral arrangement of the resonant ions. Moreover, the energies of the L_2 and L_3 edges, e.g. for terbium: 8.3 keV and 7.5 keV, respectively, correspond to wavelengths that are very suitable for diffraction studies (the wavelength in Å of radiation with an energy E in keV is $12.4/E$).

The interpretation of data on E1 (dipole) absorption events in terms of valuable atomic quantities is not straightforward. This is because the magnetism of the 4f electrons is seen to the extent that it influences the 5d band into which the ejected 2p electron is promoted.

By comparison with E1 absorption events, the interpretation of E2 (quadrupole) events, in which a 2p electron is replaced by a hole from the 4f valence shell, should be relatively straightforward. For lanthanide ions an atomic model is a realistic starting point. Such a model has been successfully used to understand the E2 contribution to the dichroic signal in the attenuation coefficient at the L_3 edge of Yb in $YbFe_2$ (Giorgetti *et al* 1995). For the configuration f^{13}, appropriate to Yb^{3+}, selection rules act to simplify the pattern of E1 and E2 contributions at the L_2 and L_3 edges, and Giorgetti *et al* (1995) obtain conclusive results on the E2 contribution largely as a result of their judicious choice for the resonant ion. For other ions the relative contributions from the E1 and E2 absorption edges are much more of an open question. Recently, van Veenendaal *et al* (1997) have addressed it, in a framework that is based on an atomic model, and have reviewed why E2 events are not clearly separated from E1 events in the attenuation coefficient. The E2 contribution to the cross-section for Bragg diffraction from $SmNi_2B_2C$ has been used by Detlefs *et al* (1997) to refine details of the orientation of the Sm moment in the antiferromagnetic state.

In the present work we use an atomic model to calculate the contribution to the resonant scattering length, f, made by an E2 absorption event. The attenuation coefficient is obtained from the imaginary part of f, evaluated for a forward-scattering geometry. An example of this type of calculation is given by Lovesey (1996), in which the attenuation coefficient for Yb^{3+} used by Giorgetti *et al* (1995) is rederived. The cross-section for Bragg diffraction is determined by $|f|^2$, and this is the topic that we now address. Our results apply to lanthanide ions with local principal axes of quantization at an arbitrary orientation with respect to the axes used to describe the geometry of the diffraction experiment.

The scattering length is defined in the next section. An idealized form of f, developed by Lovesey and Balcar (1997a), is used in section 3 to describe diffraction at the L_2 and L_3 edges. A few examples are discussed in section 4. (The idealized scattering length contains the standard sum rules used in the interpretation of circular dichroic signals in the attenuation coefficient.) A superior estimate of resonance-enhanced scattering is given in section 5, and it is illustrated in an application to terbium. In the new estimate, the scattering length contains structure coming from the core state. The cross-section for partial polarization in the primary beam is taken up in section 6, and the expression given is illustrated with a calculation of the intensity at a first-order satellite from a spiral arrangement of lanthanide ions. Partial polarization in the secondary beam is also discussed. A brief summary of our findings is found in section 7.

2. Scattering length

We consider the elastic diffraction of x-rays, in which the valence electrons of the resonant ion are in the same equilibrium (discrete) state before and after the scattering event. A state of the valence shell is labelled by μ. The quasi-discrete intermediate states of the ion are labelled by $\{\eta\}$, and they have energies $E_\eta - \mathrm{i}\gamma_\eta/2$, where $\gamma/\hbar$ is the total probability of all possible processes by which an intermediate state can decay. It is convenient to define

$\Delta = E_\eta - E_\mu$.

The primary and secondary x-rays have wave vectors $\boldsymbol{q}$ and $\boldsymbol{q}'$. The x-rays are deflected through an angle θ (=twice the Bragg angle) and $k = 2q\sin(\theta/2)$, with the primary energy $E = \hbar cq$.

Let the vectors $\{\boldsymbol{R}_0\}$ define the positions of the resonant ions. The Debye–Waller factor $\exp\{-W(\boldsymbol{k})\}$ might depend on the position of the ion in the crystal.

The mean value of the scattering length is denoted by $\langle f\rangle$, where the angular brackets indicate that an appropriate average is taken with respect to all quantities that are degenerate in f. For E close to Δ,

$$\langle f\rangle = -(qe)^2 \sum_{\boldsymbol{R}_0} \exp\{-W(\boldsymbol{k}) + \mathrm{i}\boldsymbol{k}\cdot\boldsymbol{R}_0\} \left\{ \frac{\langle Z(\mu;\mu'\!:\boldsymbol{R}_0)\rangle}{E - \Delta + (\mathrm{i}/2)\gamma} \right\}_\eta . \tag{2.1}$$

In the idealized scattering length, used in the next section, η refers to the total angular momentum, $\bar{J}$, of the core state into which the primary photon is absorbed. For the L_2 and L_3 edges $\bar{J} = \frac{1}{2}$ and $\frac{3}{2}$, respectively. Looking ahead to section 5, the scattering length used there depends on $\bar{J}$ and the associated magnetic quantum number, $\bar{M}$.

Atomic quantities associated with the valence shell enter $\langle f\rangle$ through $\langle Z(\mu;\mu'\!:\boldsymbol{R}_0)\rangle$. This is a diagonal matrix element, or a mean value, which, in general, is a sum of matrix elements $Z(\mu;\mu\!:\boldsymbol{R}_0)$ and $Z(\mu;\mu'\!:\boldsymbol{R}_0)$ weighted by factors that are determined by interactions that perturb the valence shell. We will assume that the wave function for the valence shell is taken from one J-manifold. Hence, all of the atomic quantum numbers (S, L, J and the seniority) are common in μ and μ' apart from the magnetic quantum numbers M and M'. In the calculation, the latter appear only in the Clebsch–Gordan coefficient, or $3j$-symbol, in the Wigner–Eckart theorem. The degeneracy of f with respect to the magnetic quantum numbers is removed by the action of the molecular field responsible for the spontaneous magnetic order in the crystal. Hence, the thermodynamic properties of the resonant ion appear in $\langle f\rangle$ through $3j$-symbols averaged with respect to the magnetic quantum numbers.

3. Idealized scattering length

A matrix element for E2 absorption is (Lovesey 1996)

$$Z(\mu;\mu'\!:\boldsymbol{R}_0) = \Phi \sum_K (-1)^K (2K+1)^{1/2} \begin{Bmatrix} 2 & K & 2 \\ 3 & 1 & 3 \end{Bmatrix} \sum_{m_0} \langle\mu|T^K_{m_0}|\mu'\rangle_{(xyz)} H^{(K)}_{-m_0} (-1)^{m_0}. \tag{3.1}$$

The argument of the $6j$-symbol is correct for a valence shell with angular momentum $l = 3$, and a triangle condition limits the integer K to the range $0 \leqslant K \leqslant 4$. For $l = 3$,

$$\Phi = \frac{3}{10}(q\langle 2\mathrm{p}|R^2|4\mathrm{f}\rangle)^2 \tag{3.2}$$

and, in units of the square of the Bohr radius, the radial integral $\langle 2\mathrm{p}|R^2|4\mathrm{f}\rangle \sim 0.002$. Note that Φ is proportional to E^2 and the scattering length for an E2 event is proportional to E^4. Due to this dependence on energy of the scattering length, the cross-sections at the L_2 and L_3 edges of terbium have a relative weighting that is $=(8.3/7.5)^8 = 2.5$, and the corresponding factor for samarium is 3.0.

The spherical tensor $\mathbf{H}^{(K)}$ is defined by Lovesey (1996). It depends on the polarization vectors and directions of the primary and secondary beams. Here we consider a primary beam with complete polarization perpendicular to the plane defined by $\boldsymbol{q}$ and $\boldsymbol{q}'$, the plane of

Table 1. The components of $\mathbf{C}^{(K)} \cdot \mathbf{H}^{(K)}$ are shown for $K = 0$ to $K = 4$. For each K there are two components labelled by the state of polarization in the secondary beam, namely, σ' and π'. The primary beam is purely σ-polarization. In the far left-hand column, in round brackets, there is a factor that is common to the two components. The values of $\mathbf{H}^{(K)}$ are slightly different from the definition given by Lovesey (1996). The difference is a multiplicative constant chosen to make the factor in the left-hand column a rational fraction; for $K = 0$ to $K = 4$ the constant that multiplies the original definition of $\mathbf{H}^{(K)}$ is $1/\sqrt{5}$, $1/\sqrt{10}$, $1/\sqrt{14}$, $1/\sqrt{10}$ and $1/\sqrt{70}$. The function $C_q^{(K)}(\beta, \alpha)$ is a spherical harmonic with the normalization suggested by Racah, which gives $C_0^{(0)}(\beta, \alpha) = 1$. Note that for K odd, entries are purely imaginary, and the other entries are purely real. States of linear and circular polarization are discussed in section 6, together with the corresponding cross-section.

	$\sigma'\sigma$	$\pi'\sigma$
$K = 0$ (1/10)	$\cos\theta$	0
$K = 1$ (i/20)	$\sin\theta\cos\beta$	$-\sin(\frac{3}{2}\theta + \alpha)\sin\beta$
$K = 2$ ($-1/56$)	$(1/2)\cos\theta(1 + 3\cos 2\beta)$ $+(3/2)(\cos 2\beta - 1)\cos 2\alpha$	$3\cos(\frac{3}{2}\theta + \alpha)\sin 2\beta$
$K = 3$ ($-$i/80)	$\sin\theta(3\cos\beta + 5\cos 3\beta)$	$(3/4)\sin(\frac{3}{2}\theta + \alpha)(\sin\beta + 5\sin 3\beta)$ $+(5/4)\sin(\frac{1}{2}\theta + 3\alpha)(3\sin\beta - \sin 3\beta)$
$K = 4$ ($-1/2240$)	$\cos\theta(9 + 20\cos 2\beta + 35\cos 4\beta)$ $+5(3 + 4\cos 2\beta - 7\cos 4\beta)\cos 2\alpha$	$(5/2)[\cos(\frac{3}{2}\theta + \alpha)(2\sin 2\beta + 7\sin 4\beta)$ $+7\cos(\frac{1}{2}\theta + 3\alpha)(2\sin 2\beta - \sin 4\beta)]$

scattering, since this is frequently the arrangement used in experiments. (Section 6 contains the cross-section for a primary beam with linear polarization and circular polarization.) In keeping with current usage, this state of polarization in the primary beam is labelled σ-polarization and the orthogonal case of polarization in the plane of scattering is labelled π-polarization. For our present purposes, all of the necessary values of $\mathbf{H}^{(K)}$ appear in table 1.

The atomic matrix element $\langle\mu|T^K_{m_0}|\mu'\rangle$ depends on the position of the ion in the crystal through the orientation of its axes of quantization relative to the axes for the geometry of the experiment, in which $\mathbf{H}^{(K)}$ is calculated. In general, these two sets of axes will not coincide, and the local principal axes of quantization for each ion in the magnetic unit cell will be different.

The axes for the geometry of the experiment are denoted by (x, y, z). Following the convention adopted by Lovesey and Collins (1996), the unit vectors $\hat{\boldsymbol{x}}$, $\hat{\boldsymbol{y}}$ and $\hat{\boldsymbol{z}}$ are

$$2\sin(\theta/2)\hat{\boldsymbol{x}} = \hat{\boldsymbol{q}}' - \hat{\boldsymbol{q}} \tag{3.3a}$$

$$2\cos(\theta/2)\hat{\boldsymbol{y}} = \hat{\boldsymbol{q}}' + \hat{\boldsymbol{q}} \tag{3.3b}$$

and

$$\sin(\theta)\hat{\boldsymbol{z}} = \hat{\boldsymbol{q}}' \times \hat{\boldsymbol{q}}. \tag{3.3c}$$

The axes of quantization for an ion relative to (x, y, z) are defined by three Euler angles α, β and γ, and for these we follow the convention used by Judd (1975). The principal axis of quantization for an ion is

$$\boldsymbol{m} = \hat{\boldsymbol{x}}\cos\alpha\sin\beta + \hat{\boldsymbol{y}}\sin\alpha\sin\beta + \hat{\boldsymbol{z}}\cos\beta. \tag{3.4}$$

Let us now turn to the relation between the atomic matrix elements in the two sets of axes.

The matrix element of the atomic spherical tensor $T^K_{m_0}$ in the local principal axes of magnetic quantization is denoted simply by $\langle\mu|T^K_{m_0}|\mu'\rangle$. The corresponding matrix element

in the axes (x, y, x), which is required in the formula (3.1), is denoted by $\langle\mu|T^K_{m_0}|\mu'\rangle_{(xyz)}$. One finds

$$\langle\mu|T^K_{m_0}|\mu'\rangle_{(xyz)} = \sum_Q \langle\mu|T^K_Q|\mu'\rangle \mathcal{D}^{(K)}_{Qm_0}(-\gamma, -\beta, -\alpha) \tag{3.5}$$

where $\mathcal{D}^{(K)}$ is an element of the rotation matrix. We will assume that, in the local principal axes of quantization, the atomic matrix element is diagonal with respect to the magnetic quantum numbers. (This assumption is not valid if the perturbation of the valence shell by the ligand crystal-field potential is very strong.) Setting $M = M'$ in (3.5) means that on the right-hand side all terms in the sum are zero except the term with $Q = 0$. One then finds

$$\langle\mu|T^K_{m_0}|\mu'\rangle_{(xyz)} = C^{(K)}_{m_0}(\beta, \alpha)\langle\mu|T^K_0|\mu'\rangle \tag{3.6}$$

in which $C^{(K)}_{m_0}(\beta, \alpha)$ is a spherical harmonic with a normalization such that $C^{(0)}_0(\beta, \alpha) = 1$. Using (3.6) in (3.1) one is left to calculate

$$\sum_{m_0} C^{(K)}_{m_0}(\beta, \alpha) H^{(K)}_{-m_0}(-1)^{m_0} = \mathbf{C}^{(K)} \cdot \mathbf{H}^{(K)} \tag{3.7}$$

and our results are given in table 1. In calculating the entries we have used the relation

$$H^{(K)}_{-m_0} = (-1)^{K+m_0}\{H^{(K)}_{m_0}\}^*.$$

Notice that, with the assumed simple wave function for the valence shell, the matrix element (3.1) depends on two of the three Euler angles. We will have more to say about the entries in table 1 in the next section.

The atomic matrix element on the right-hand side of (3.6) is taken to be

$$\langle\mu|T^K_0|\mu\rangle = (-1)^{J-M}\begin{pmatrix} J & K & J \\ -M & 0 & M \end{pmatrix}(\nu SLJ||T(K:\bar{J})||\nu SLJ). \tag{3.8}$$

The reduced matrix element in (3.8) is given by Lovesey and Balcar (1997a) in terms of Racah unit tensors. In the next section we provide some illustrative examples of the reduced matrix elements, calculated for lanthanide ions. The quantum numbers ν, S, L and J are determined by Hund's rules. As is well known, the ground states of lanthanide ions are very pure, i.e. a state determined by Hund's rules is a good approximation to the ground state.

It is appropriate to comment on an aspect of our use of Racah unit tensors that reflects both on the sign of the magnetic quantum number taken in (3.8), and the definition of a state constructed with holes. The absorption event of interest to us involves a photo-emitted electron taking up a state in the valence shell. In consequence, the atomic matrix elements in the scattering length, f, include empty states in the valence shell. Fortunately, matrix elements for empty states and occupied states are very simply related. So, in our theoretical framework, f is a mean value constructed with a wave function of the electrons in the valence shell rather than the holes in the shell, in which there is less physical interest.

We explore the relation between empty and occupied states in terms of matrix elements of the Racah unit tensor $W^{(ab)K}$, where a and b are the ranks of the spin and orbital operators, and the integer K satisfies the triangle condition $|a - b| \leqslant K \leqslant (a + b)$. Let us denote the eigenvectors of the empty and occupied states of the nl-shell by $|\text{emp.}\rangle$ and $|\text{occ.}\rangle$. Evidently,

$$\sum |\text{emp.}\rangle\langle\text{emp.}| + \sum |\text{occ.}\rangle\langle\text{occ.}| = 1.$$

The wave function $|\mu\rangle$ of the electrons in the shell is constructed from $\{|\text{occ.}\rangle\}$. Similarly, from $\{|\text{emp.}\rangle\}$, construct $|\Phi_{\text{emp}}\rangle$. For the closed shell the wave function of the electrons is

denoted by $|\Phi\rangle$. With these definitions, and the foregoing statement of closure for the states of the valence shell, we are led to the identity

$$\langle\Phi_{\rm emp}|W^{(ab)K}|\Phi_{\rm emp}\rangle = \langle\Phi|W^{(ab)K}|\Phi\rangle - \langle\mu|W^{(ab)K}|\mu\rangle. \tag{3.9}$$

The diagonal matrix element for a closed shell has the following properties. For $a+b>0$,

$$\langle\Phi|W^{(ab)K}|\Phi\rangle = 0$$

and for $a+b=0$ the matrix element is proportional to $2(2l+1)$. Thus, for $a+b>0$ the matrix element involving empty states, that naturally arises in f, is equal in magnitude and opposite in sign to the matrix element for the occupied (electron) states. For $a+b=0$ the matrix element for the empty states is proportional to $2(2l+1)-n_{\rm e}=n_{\rm h}$.

For $a+b>0$, the matrix elements with $n_{\rm h}$ empty states, found in f, are constructed from the matrix elements with $n_{\rm e}=2(2l+1)-n_{\rm h}$ electrons, namely, $\langle\mu|W^{(ab)K}|\mu\rangle$. The quantum numbers seniority, S and L for the $n_{\rm h}$ empty states and the $n_{\rm e}$ electron states are the same; $|l^{n_{\rm h}}\nu SL\rangle$ and $|l^{n_{\rm e}}\nu SL\rangle$ with $n_{\rm h}+n_{\rm e}=2(2l+1)$ are often called conjugate configurations, or states. We separately consider $a+b=$ even integer and $a+b=$ odd integer. For $a+b$ even the minus sign in (3.9) is included in the values of $\langle\mu|W^{(ab)K}|\mu\rangle$ that we have tabulated in previous papers. Hence, for this case, use of our tables gives the correct result for f. We have decided to deal with $a+b$ odd in a different way, and a minus sign is not included in the tabulated quantities. Our reason for not including a minus sign is to adhere to a standard definition of a hole state, which amounts to defining the saturated ion by $M=+J$ or $-J$. We later have more to say about the topic of hole states. For the moment, though, we note that for a non-zero matrix element it is necessary that $a+b+K$ is an even integer, and matrix elements with $|\mu\rangle=|JM\rangle$ and $|\mu\rangle=|J,-M\rangle$ satisfy

$$\langle J,-M|W^{(ab)K}|J,-M\rangle = (-1)^K\langle JM|W^{(ab)K}|JM\rangle.$$

Hence, for a one-component wave function and $a+b$ odd, there is a one-to-one correspondence between a state with quantum numbers $J,-M$ appearing in f and a state of the electrons labelled by J,M.

Our adopted definition of a hole state, $|h\rangle$, constructed from the empty states of a shell, uses a correspondence with a state of the occupied (electron) states, $|\mu\rangle$, such that mean values of the spin and orbital angular momentum operators satisfy

$$\langle h|\boldsymbol{S}|h\rangle = \langle\mu|\boldsymbol{S}|\mu\rangle \qquad \text{and} \qquad \langle h|\boldsymbol{L}|h\rangle = \langle\mu|\boldsymbol{L}|\mu\rangle.$$

We recall that a matrix element of $\boldsymbol{S}$ ($\boldsymbol{L}$) is constructed with $W^{(10)1}$ ($W^{(01)1}$). Also, $\boldsymbol{S}$ and $\boldsymbol{L}$ are time-odd operators; for example,

$$\theta^{-1}\boldsymbol{S}\theta = -\boldsymbol{S}$$

where θ is the time-reversal operator. In view of (3.9), the above-mentioned one-to-one correspondence is realized with

$$|h\rangle = \theta|\Phi_{\rm emp}\rangle$$

since, following Lovesey (1986),

$$\langle h|\boldsymbol{S}|h\rangle = \langle\Phi_{\rm emp}|\theta^{-1}\boldsymbol{S}\theta|\Phi_{\rm emp}\rangle^* = -\langle\Phi_{\rm emp}|\boldsymbol{S}^+|\Phi_{\rm emp}\rangle = -\langle\Phi_{\rm emp}|\boldsymbol{S}|\Phi_{\rm emp}\rangle = \langle\mu|\boldsymbol{S}|\mu\rangle$$

i.e. the hole state is created by the time-reversal operator from the empty state. If one uses the eigenstates $|JM\rangle$ of the angular momentum

$$|\Phi_{\rm emp}\rangle = \sum_{JM} Q(J,M)|JM\rangle$$

and the set of numbers $Q(J, M)$ define $|\Phi_{\rm emp}\rangle$. We then find

$$|h\rangle = \sum_{JM} Q^*(J, M)(-1)^{J+M}|J, -M\rangle.$$

For the special case in which all but one of the $Q(J, M)$ are zero, we may take

$$|h\rangle = (-1)^{J+M}|J, -M\rangle$$

and, since $J + M$ is an integer,

$$\langle h|\boldsymbol{S}|h\rangle = \langle J, -M|\boldsymbol{S}|J, -M\rangle.$$

The correspondence expressed by this result is the motivation for our treatment of the odd-rank Racah unit tensors and their matrix elements. We rely on an external magnetic field to define the axis of quantization for the electron states.

Table 2. The entries in the table are analytic expressions for $F_J(K)$ defined in (3.10) as the ratio of two $3j$-symbols. The denominator is the value of the M-polynomial in the numerator evaluated for $M = J$. Hence, for a saturated magnetic ion, $F_J(K)$ has a magnitude of one, for all K.

$K = 1$	$\langle M\rangle/J$
$K = 2$	$\langle 3M^2 - J(J+1)\rangle/\{J(2J-1)\}$
$K = 3$	$\langle M\{5M^2 + 1 - 3J(J+1)\}\rangle/\{J(J-1)(2J-1)\}$
$K = 4$	$\langle 35M^4 + 5M^2\{5 - 6J(J+1)\} + 3J(J^2-1)(J+2)\rangle/\{2J(J-1)(2J-1)(2J-3)\}$

The thermodynamic properties of an ion that arise in $\langle f\rangle$ derive from the $3j$-symbols averaged with respect to the M-degeneracy. It proves convenient to use a function

$$F_J(K) = \left\langle (-1)^{J-M}\begin{pmatrix} J & K & J \\ -M & 0 & M\end{pmatrix}\right\rangle \begin{pmatrix} J & K & J \\ -J & 0 & J\end{pmatrix}^{-1} \tag{3.10}$$

in which the angular brackets denote the thermal average with respect to the $2J + 1$ values of M. One finds $F_J(0) = 1$, and analytic expressions for $F_J(K)$ with $K > 0$ are found in table 2.

In the event that in order to achieve a fully realistic description of the valence shell one needs to use a wave function that is a linear combination of several states, each with a different value of M, the mean value of $Z(\mu; \mu'{:}\,\boldsymbol{R}_0)$ will be a linear combination of quantities proportional to

$$(\nu SLJ||T(K{:}\,\bar{J})||\nu SLJ)\sum_{Q}(-1)^{J-M}\begin{pmatrix} J & K & J \\ -M & Q & M'\end{pmatrix}\mathcal{D}^{(K)}_{Qm_0}(-\gamma, -\beta, -\alpha). \tag{3.11}$$

From this expression it is evident that, for states drawn from a single J-manifold, in $\langle f\rangle$ the reduced atomic matrix element is a common factor. So, while use of a simple wave function, with only one M-state, might lead in $\langle f\rangle$ to an approximate description of the thermodynamic properties of the resonant ion, the specification of the atomic state is completely correct.

Table 3. The function $\Psi_\mu(K)$ is defined in equation (4.2). Apart from the factors listed in the caption to table 1, the quantities listed in the table are the coefficients of $F_J(K)$ in (4.2), evaluated for the tripositive lanthanide ions. The quantum numbers in the label μ are determined by Hund's rules.

Ce^{3+} f^1 $n_h = 13$ $^2F_{5/2}$		Dy^{3+} f^9 $n_h = 5$ $^6H_{15/2}$	
$K = 0$	$\frac{13}{42}[(2\bar{J}_\pm + 1) \pm \frac{8}{39}]$	$K = 0$	$\frac{5}{42}[(2\bar{J}_\pm + 1) \pm \frac{2}{3}]$
$K = 1$	$\frac{20}{441}[(2\bar{J}_\pm + 1) \mp \frac{29}{10}]$	$K = 1$	$\frac{5}{63}[(2\bar{J}_\pm + 1) \pm \frac{6}{5}]$
$K = 2$	$\frac{2}{49}[-(2\bar{J}_\pm + 1) \pm \frac{31}{9}]$	$K = 2$	$\frac{1}{21}[-(2\bar{J}_\pm + 1) \pm \frac{4}{3}]$
$K = 3$	$\frac{5}{294}[(2\bar{J}_\pm + 1) \mp \frac{68}{15}]$	$K = 3$	$[\pm\frac{1}{63}]$
$K = 4$	$\frac{11}{882}[-(2\bar{J}_\pm + 1) \pm \frac{76}{11}]$	$K = 4$	$\frac{2}{63}[(2\bar{J}_\pm + 1) \mp \frac{5}{2}]$
Pr^{3+} f^2 $n_h = 12$ $^3H_4$		Ho^{3+} f^{10} $n_h = 4$ $^5I_8$	
$K = 0$	$\frac{2}{7}[(2\bar{J}_\pm + 1) \pm \frac{1}{3}]$	$K = 0$	$\frac{2}{21}[(2\bar{J}_\pm + 1) \pm 1]$
$K = 1$	$\frac{8}{105}[(2\bar{J}_\pm + 1) \mp \frac{82}{45}]$	$K = 1$	$\frac{2}{21}[(2\bar{J}_\pm + 1) \pm \frac{16}{15}]$
$K = 2$	$\frac{104}{2475}[-(2\bar{J}_\pm + 1) \pm \frac{12}{13}]$	$K = 2$	$\frac{2}{105}[-(2\bar{J}_\pm + 1) \pm 1]$
$K = 3$	$[\pm\frac{884}{17325}]$	$K = 3$	$\frac{1}{42}[-(2\bar{J}_\pm + 1) \pm \frac{4}{5}]$
$K = 4$	$\frac{2}{99}[(2\bar{J}_\pm + 1) \mp \frac{20}{3}]$	$K = 4$	$\frac{1}{42}[(2\bar{J}_\pm + 1) \pm \frac{4}{3}]$
Nd^{3+} f^3 $n_h = 11$ $^4I_{9/2}$		Er^{3+} f^{11} $n_h = 3$ $^4I_{15/2}$	
$K = 0$	$\frac{11}{42}[(2\bar{J}_\pm + 1) \pm \frac{14}{33}]$	$K = 0$	$\frac{1}{14}[(2\bar{J}_\pm + 1) \pm \frac{4}{3}]$
$K = 1$	$\frac{1}{11}[(2\bar{J}_\pm + 1) \mp \frac{94}{77}]$	$K = 1$	$\frac{2}{21}[(2\bar{J}_\pm + 1) \pm \frac{19}{15}]$
$K = 2$	$\frac{2}{121}[-(2\bar{J}_\pm + 1) \mp \frac{28}{15}]$	$K = 2$	$\frac{2}{105}[(2\bar{J}_\pm + 1) \pm 1]$
$K = 3$	$\frac{28}{1573}[-(2\bar{J}_\pm + 1) \pm \frac{35}{18}]$	$K = 3$	$\frac{1}{42}[-(2\bar{J}_\pm + 1) \mp \frac{4}{5}]$
$K = 4$	$\frac{68}{4719}[(2\bar{J}_\pm + 1) \pm \frac{77}{17}]$	$K = 4$	$\frac{1}{42}[-(2\bar{J}_\pm + 1) \pm \frac{4}{3}]$
Pm^{3+} f^4 $n_h = 10$ $^5I_4$		Tm^{3+} f^{12} $n_h = 2$ $^3H_6$	
$K = 0$	$\frac{5}{21}[(2\bar{J}_\pm + 1) \pm \frac{7}{15}]$	$K = 0$	$\frac{1}{21}[(2\bar{J}_\pm + 1) \pm \frac{5}{3}]$
$K = 1$	$\frac{4}{45}[(2\bar{J}_\pm + 1) \mp \frac{60}{77}]$	$K = 1$	$\frac{5}{63}[(2\bar{J}_\pm + 1) \pm \frac{8}{5}]$
$K = 2$	$\frac{28}{1815}[(2\bar{J}_\pm + 1) \mp \frac{28}{15}]$	$K = 2$	$\frac{1}{21}[(2\bar{J}_\pm + 1) \pm \frac{4}{3}]$
$K = 3$	$\frac{28}{1815}[-(2\bar{J}_\pm + 1) \mp \frac{35}{18}]$	$K = 3$	$[\mp\frac{1}{63}]$
$K = 4$	$\frac{476}{42471}[-(2\bar{J}_\pm + 1) \pm \frac{77}{17}]$	$K = 4$	$\frac{2}{63}[-(2\bar{J}_\pm + 1) \mp \frac{5}{2}]$
Sm^{3+} f^5 $n_h = 9$ $^6H_{5/2}$		Yb^{3+} f^{13} $n_h = 1$ $^2F_{7/2}$	
$K = 0$	$\frac{3}{14}[(2\bar{J}_\pm + 1) \pm \frac{4}{9}]$	$K = 0$	$\frac{1}{42}[(2\bar{J}_\pm + 1) \pm 2]$
$K = 1$	$\frac{10}{147}[(2\bar{J}_\pm + 1) \mp \frac{23}{45}]$	$K = 1$	$\frac{1}{21}[(2\bar{J}_\pm + 1) \pm 2]$
$K = 2$	$\frac{13}{441}[(2\bar{J}_\pm + 1) \pm \frac{12}{13}]$	$K = 2$	$\frac{1}{21}[(2\bar{J}_\pm + 1) \pm 2]$
$K = 3$	$[\mp\frac{221}{9261}]$	$K = 3$	$\frac{1}{42}[(2\bar{J}_\pm + 1) \pm 2]$
$K = 4$	$\frac{13}{2646}[-(2\bar{J}_\pm + 1) \mp \frac{20}{3}]$	$K = 4$	$\frac{1}{42}[(2\bar{J}_\pm + 1) \pm 2]$

4. Lanthanide ions

For the chosen model of a resonant lanthanide ion the mean value of the matrix element Z in $\langle f \rangle$ can be written in the form

$$\langle Z(\mu;\mu{:}\,\boldsymbol{R}_0)\rangle = \Phi \sum_K \mathbf{C}^{(K)} \cdot \mathbf{H}^{(K)} \Psi_\mu(K). \tag{4.1}$$

Table 3. (Continued)

Eu^{3+}	f^6	$n_h = 8$	$^7F_0$
$K = 0$	$\frac{4}{21}[(2\bar{J}_\pm + 1) \pm \frac{1}{3}]$		
Gd^{3+}	f^7	$n_h = 7$	$^8S_{7/2}$
$K = 0$	$\frac{1}{6}[(2\bar{J}_\pm + 1)$	]	
$K = 1$	$[\pm\frac{2}{9}]$		
Tb^{3+}	f^8	$n_h = 6$	$^7F_6$
$K = 0$	$\frac{1}{7}[(2\bar{J}_\pm + 1) \pm \frac{1}{3}]$		
$K = 1$	$\frac{1}{21}[(2\bar{J}_\pm + 1) \pm \frac{8}{3}]$		
$K = 2$	$\frac{1}{21}[-(2\bar{J}_\pm + 1) \pm 2]$		
$K = 3$	$\frac{1}{42}[(2\bar{J}_\pm + 1) \mp 2]$		
$K = 4$	$\frac{1}{42}[-(2\bar{J}_\pm + 1) \pm 2]$		

The scalar product of $\mathbf{C}^{(K)}$ and $\mathbf{H}^{(K)}$ is the subject of table 1. The entries depend on two Euler angles, α and β, used to define the local principal axes of quantization of the resonant ion. In general, these angles will depend on the position of the ion in the magnetic unit cell.

The quantity that contains the atomic and thermodynamic properties of the ion is

$$\Psi_\mu(K) = (-1)^K (2K+1)^{1/2} \begin{pmatrix} J & K & J \\ -J & 0 & J \end{pmatrix} \begin{Bmatrix} 2 & K & 2 \\ 3 & 1 & 3 \end{Bmatrix} (\mu||T(K{:}\,\bar{J})||\mu) F_J(K) \qquad (4.2)$$

and it is defined in accord with the general expression for an E2 event (3.1), and (3.6) and (3.8). The dependence of Ψ on the core state arises from the dependence on $\bar{J}$ of the reduced matrix element. Looking at (3.8) reveals that, in (4.2) the product of the $3j$-symbol and the reduced matrix element is equal to the diagonal matrix element of T_0^K evaluated for the state μ and the value $M = J$. The label μ represents the quantum numbers required to define the state obtained from Hund's rules. Using for the reduced matrix element in (4.2) results given by Lovesey and Balcar (1997a) we have obtained the entries in table 3, which enable one to construct $\Psi_\mu(K)$.

By way of illustration of the use of the entries in tables 1–3, let us consider the entries for f^7. Of course, having a half-filled valence shell, this ion has a particularly simple scattering length. For the matrix element in the numerator of the mean value of the resonant scattering length we obtain

$$\langle Z \rangle = \frac{1}{6}\Phi \left\{ (2\bar{J}+1) C_0^{(0)} H_0^{(0)} \pm \frac{4}{3} \mathbf{C}^{(1)} \cdot \mathbf{H}^{(1)} F_{7/2}(1) \right\}. \qquad (4.3)$$

Here, the plus sign refers to the L_3 absorption edge ($\bar{J} = \frac{3}{2}$) and the minus sign refers to the L_2 absorption edge ($\bar{J} = \frac{1}{2}$).

In the formula for $\langle f \rangle$ it is the sum over $\boldsymbol{R}_0$ and the spatial coherence factor $\exp(\mathrm{i}\boldsymbol{k}\cdot\boldsymbol{R}_0)$ that generate the Bragg condition for $\boldsymbol{k}$. If the Euler angles are independent of $\boldsymbol{R}_0$ it follows that all of the terms in the sum over K in (4.1) can contribute to the intensity of a Bragg peak. Looking at (4.3), we see that this will mean contributions from terms with $K = 0$ and 1. When the secondary beam is analysed for π-polarization, the entries in table 1 labelled $\pi'\sigma$ are appropriate, and we find

$$|\langle f \rangle|^2_{\pi'\sigma} = \left\{ \frac{1}{90}(qe)^2 \Phi \right\}^2 \frac{[F_{7/2}(1) \sin(\frac{3}{2}\theta + \alpha) \sin\beta]^2}{[(E-\Delta)^2 + (\frac{1}{2}\Gamma)^2]}. \qquad (4.4)$$

The intensity at the L_2 and L_3 edges is the same, apart from differences in E, Δ and Γ. It is interesting to note that the scattering is zero if the magnetic axis is perpendicular to the plane of scattering. By referring to table 2 we see that $F_J(1)$ is the normalized magnetic moment of the resonant ion. For the $\sigma'\sigma$-channel of scattering the result for $|\langle f\rangle|^2$ is slightly richer in its structure, that is,

$$|\langle f\rangle|^2_{\sigma'\sigma} = \left\{\frac{1}{60}(qe)^2\Phi\right\}^2\left\{\left[(E-\Delta)(2\bar{J}+1)\cos\theta \pm \frac{\Gamma}{3}F_{7/2}(1)\sin\theta\cos\beta\right]^2 + \left[\frac{\Gamma}{2}(2\bar{J}+1)\cos\theta \mp \frac{2}{3}(E-\Delta)F_{7/2}(1)\sin\theta\cos\beta\right]^2\right\} \times \left[(E-\Delta)^2 + \left(\frac{1}{2}\Gamma\right)^2\right]^{-2}. \tag{4.5}$$

Evidently, the intensity is different at the L_2 and L_3 absorption edges, for reasons other than differences at the two edges in E, Δ and Γ. The intensity is independent of the magnetic moment of the ion if this lies in the plane of scattering. On a general note, when the polarization in the secondary beam of x-rays is not analysed, the observed intensity is the sum of the intensities in the two scattering channels.

Next consider the situation in which the arrangement of the magnetic moments is a simple spiral with a pitch that is incommensurate with the chemical unit cell of the crystal. For such an arrangement one anticipates Bragg reflections that are satellites to the Bragg reflections indexed by the chemical crystal lattice. No such satellite reflections will be observed if the axis of the spiral is perpendicular to the plane of scattering. For, in this case, the moments are contained in the plane and, according to (3.4), $\beta = \pi/2$ and α is the turn angle between planes in the spiral arrangement of the moments. With this choice of β the $\sigma'\sigma$-intensity contains no information on the magnetic moments, and the turn angle in (4.4) does not depend on the x- and y-components of $\boldsymbol{R}_0$ that occur in the spatial coherence factor.

As a second case, let us consider the axis of the spiral in the plane of scattering. Now β is the turn angle and a first-order satellite can be observed in both the $\sigma'\sigma$- and $\pi'\sigma$-channels of scattering. For f^7 there are no satellites with an order larger than one, because the maximum value of $K = 1$. The intensity for $\sigma'\sigma$-scattering at the satellite reflection is found from (4.5):

$$|\langle f\rangle|^2_{\sigma'\sigma} = \left\{\frac{1}{180}(qe)^2\Phi\right\}^2 \frac{[F_{7/2}(1)\sin\theta]^2}{[(E-\Delta)^2 + (\frac{1}{2}\Gamma)^2]}. \tag{4.6}$$

The corresponding expression for $\pi'\sigma$-scattering is the same except that $\sin\theta$ is replaced by $\sin(\frac{3}{2}\theta + \alpha)$. Hence, $\pi'\sigma$-scattering depends on the orientation of the axis of the spiral with respect to $\boldsymbol{k}$, and, should the two vectors be aligned, $\alpha = \pi/2$. The intensity of the first-order satellite does not depend on $\bar{J}$.

Entries in table 1 have been expressed in terms of $\cos n\beta$ and $\sin n\beta$ to facilitate the identification of contributions to a satellite of order n. The maximum value of n is K, and n is even or odd according to whether K is even or odd. One should notice that components with K odd are $\pi/2$ out of phase with the K-even components.

The dependence of the mean scattering length on the thermodynamic state of the resonant ion is carried by the quantities $F_J(K)$, found in table 2. From their definition, these quantities have a magnitude of one for the saturated state, and thus each term in the sum over K in (4.1) for this state has an equal thermodynamic weight. Moreover, the definition

of $F_J(K)$ is such that for $K > 0$ the trace of the polynomial in M is zero. From this property we conclude that $F_J(K) = 0$ at an infinite temperature.

By way of an orientation to the magnitude of $F_J(K)$ at a relatively high temperature, just less than the critical temperature T_c below which there is spontaneous magnetic order, we appeal to the molecular-field model. The Heisenberg exchange interaction responsible for the spontaneous ordering is assumed to be isotropic in spin space, and we do not include single-site anisotropy energies. First, let us recall the well-known result

$$F_J(1) = (J+1)\left\{10\left(\frac{T_c}{T} - 1\right)\Big/ 3\{2J(J+1)+1\}\right\}^{1/2} \tag{4.7}$$

where T is the temperature. For $K > 1$ we find that $F_J(K)$ is proportional to $F_J(1)$ raised to the power K, a result that might be anticipated. Specifically

$$F_J(2) = \frac{3(2J+3)}{10(J+1)}\{F_J(1)\}^2 \tag{4.8}$$

and

$$F_J(3) = \frac{3}{10}\frac{\{2J(J+1)+1\}\{3J(J+1)-1\}\{F_J(1)\}^3}{(J-1)(2J-1)(J+1)^2}. \tag{4.9}$$

From these findings we conclude that, at a temperature close to T_c, where $F_J(1) \ll 1$, the high-order ($K > 1$) terms in (4.1) have by comparison to $F_J(1)$ a very strong dependence on temperature and a small weight.

The entries in table 3 can be interpreted in terms of various atomic quantities. This might have some merit for the low-order terms in K because the atomic quantities are relatively simple and have a genuine physical appeal. However, for $K > 2$ the atomic quantities are complicated objects, made up of high powers of the orbital angular momentum operator, and thus are less amenable to interpretation by physical intuition.

For an E2 absorption event and a valence shell with angular momentum $l = 3$,

$$\Psi_\mu(0) = \frac{1}{42}\left\{(2\bar{J}+1)n_{\rm h} \pm \frac{4}{3}\left\langle\sum \boldsymbol{s}\cdot\boldsymbol{l}\right\rangle\right\}. \tag{4.10}$$

Here, $n_{\rm h}$ is the number of holes in the valence shell, and $\langle\sum \boldsymbol{s}\cdot\boldsymbol{l}\rangle$ is the mean value of the spin–orbit operator of the holes. The corresponding expression for $\Psi_\mu(1)$ contains the reduced matrix elements of the spin (S), orbital angular momentum (L) and magnetic dipole-(T) operators. One finds

$$\Psi_\mu(1) = \frac{1}{63}F_J(1)\left\{\frac{J}{(J+1)(2J+1)}\right\}^{1/2} \times \{(2\bar{J}+1)(\mu||L||\mu) \pm 4[(\mu||S||\mu) + 3(\mu||T||\mu)]\}. \tag{4.11}$$

As an example of the use of this result let us consider Tb^{3+}. Hund's rules give $L = S = 3$ and $J = 6$, and the reduced matrix elements are

$$(\mu||L||\mu) = (\mu||S||\mu) = (273/2)^{1/2} \qquad \text{and} \qquad (\mu||T||\mu) = -\frac{1}{9}(\mu||L||\mu).$$

Inserting these values in (4.11), we obtain the entry in table 3. Lastly,

$$\Psi_\mu(2) = \frac{2}{315}F_J(2)\left\{\frac{J(2J-1)}{(J+1)(2J+1)(2J+3)}\right\}^{1/2} \times \left\{(2\bar{J}+1)(\mu||Q||\mu) \pm \frac{2}{5}[10(\mu||P||\mu) + 3(\mu||R||\mu)]\right\}. \tag{4.12}$$

In this result, Q is the quadrupole operator for orbital angular momentum while P and R, like T in (4.11), combine spin and orbital angular momentum operators; complete details are found in Lovesey and Balcar (1997b).

A few entries in table 3 warrant some comments. First, the null values for Eu^{3+} and $K > 0$ are a consequence of the null value for J. Similarly, there are just two entries for Gd^{3+} because it has $L = 0$.

The last feature of table 3 that we comment on is the absence in four ions of a term $2\bar{J} + 1$ for $K = 3$. The origin of this feature is a null value for the Racah unit tensor with an orbital angular momentum of rank 3 and $n_h = 2$, 5, 9 and 12. On going beyond the specification of the valence shell by Hund's rules, and including the full multiplet, small amounts of non-zero unit tensors contribute to the coefficient of $2\bar{J} + 1$ (Carra 1997). For lanthanide ions such effects are usually small corrections to the results obtained using a state specified by Hund's rules, i.e. the valence states have a high purity. To round off this comment, let us look at the mean values of the operators S, L and T for Tb^{3+}. Using the previously given reduced matrix elements, the mean values for the state specified by Hund's rules and $M = J$ are $\langle S\rangle = \langle L\rangle = 3$ and $\langle T\rangle = -1/3$. These results are compared with values obtained from a calculation including the full multiplet and unjustified values of the Slater integrals (Teramura *et al* 1996), namely, $\langle S\rangle = 2.943$, $\langle L\rangle = 3.057$ and $\langle T\rangle = -0.243$. It is notable that, for this particular case, the departure in $\langle T\rangle$ is as large as 27%, whereas the departures in $\langle S\rangle$ and $\langle L\rangle$ are indeed small.

5. Core-level structure in the scattering length

The results in the previous section are based on an idealized scattering length. In this approximation the resonant denominator in $\langle f\rangle$ is characterized by two constants, Δ and Γ. The numerator, or the integrated weight, is calculated without approximation for an atomic model of the valence shell. It is assumed, in this picture of events, that $\bar{J}$ is a good quantum number, which uniquely labels the resonant contributions for a given core state.

An improved picture of events is obtained by allowing for structure in the resonant contribution to $\langle f\rangle$ derived by lifting its degeneracy with respect to the magnetic quantum number for the hole in the core state, $\bar{M}$. In this case, for a given $\bar{J}$ one admits $2\bar{J} + 1$ resonant contributions that add coherently for a particular channel of scattering. The sum of the weights attached to the $2\bar{J} + 1$ contributions equals the weight predicted by the idealized scattering length. Also, the weight in the contribution labelled by $\bar{J}$ and $\bar{M}$ is again expressed in terms of Racah unit tensors for the ground state of the valence shell. Now, however, the unit tensors are nested in a sum, and their rank is not tied to the rank of the spherical tensor $\mathbf{H}^{(K)}$, as it is in the previously reported work. The details of the theory are set out by Lovesey (1997).

In the remainder of this section we explore the theory applied to the E2 contribution to $\langle f\rangle$, and evaluate it for Bragg diffraction at a first-order satellite from a spiral arrangement of the resonant ions. To this end we refer back to (3.6), to learn that with a unit tensor of rank x there is a spherical harmonic $C^{(x)}_{m_0}(\beta, \alpha)$. A first-order satellite receives contributions from odd-rank spherical harmonics, as we saw in section 4. Hence, in the matrix element $Z(\mu; \mu: \boldsymbol{R}_0)$ the Bragg condition selects terms with x odd. Another important aspect of the calculation is that each contribution of rank x is weighted by a thermal factor $F_J(x)$. It has been shown that at an elevated temperature the magnitude of the thermal factors decrease strongly with increasing rank. We limit the subsequent discussion to the dominant thermal factor, namely the rank-one factor, since spiral arrangements of the ions in rare-earth metals occur in a window of temperature immediately below the ordering temperature

(Jensen and Mackintosh 1991). Consequently, for our immediate purpose the scattering length is proportional to $F_J(1)$ and, furthermore, the orientation factors in it are derived from $C^{(1)}_{m_0}(\beta,\alpha)$.

Using η to denote the quantum labels of the core hole, one finds

$$\langle Z(\mu;\mu:\boldsymbol{R}_0)\rangle_\eta = \Phi F_J(1)\sum_{Km_0}(2K+1)^{1/2}C^{(1)}_{m_0}(\beta,\alpha)H^{(K)}_{-m_0}\mathcal{S}^{(K)}_{m_0}(\eta) \tag{5.1}$$

where

$$\begin{aligned}\mathcal{S}^K_{m_0}(\eta) = -(2\bar{J}+1)\sqrt{3}\sum_r(2r+1)(-1)^{\bar{J}-\bar{M}}&\begin{pmatrix}\bar{J} & r & \bar{J}\\ -\bar{M} & 0 & \bar{M}\end{pmatrix}\begin{pmatrix}K & r & 1\\ -m_0 & 0 & m_0\end{pmatrix}\\ &\times\sum_{ab}\langle\mu|W^{(ab)1}|\mu\rangle(2a+1)(2b+1)\sum_y(2y+1)\begin{Bmatrix}K & r & 1\\ a & b & y\end{Bmatrix}\\ &\times\begin{Bmatrix}2 & 3 & 1\\ 2 & 3 & 1\\ K & b & y\end{Bmatrix}\begin{Bmatrix}1/2 & \bar{J} & 1\\ 1/2 & \bar{J} & 1\\ a & r & y\end{Bmatrix}.\end{aligned} \tag{5.2}$$

In this expression the matrix element of the unit tensor $W^{(ab)1}$ is evaluated for $M = J$, and the arguments of the nj-symbols have been assigned values appropriate to an E2 absorption event and a 4f valence shell.

The $2\bar{J}+1$ degeneracy is lifted by an exchange interaction which acts on the spin of the ejected electron, i.e. the exchange energy is proportional to $g-1$ where g is the Landé factor. For $\bar{J} = 1 \pm \frac{1}{2}$ one finds

$$\Delta(\bar{M}) = \pm\frac{1}{3}\bar{M}\Delta_0 \tag{5.3}$$

where Δ_0 sets the size of the exchange interaction, and the energy of the absorption edge is chosen as the origin of the energy scale. At present Δ_0 is a free parameter.

Table 4. The matrix element $\langle Z\rangle_\eta$ to be used in (5.1) is obtained by multiplying the entries in the table by $\Phi F_J(1)/1764$. The numerical values are appropriate for Tb^{3+}, f^8 with $S = L = 3$ and $J = 6$.

	$\sigma'\sigma$	$\pi'\sigma$
L_2	$-(1/5)[10\bar{M}\cos\theta + 7i\sin\theta]\cos\beta$	$(1/5)[6\bar{M}\cos(\frac{3}{2}\theta+\alpha) + 7i\sin(\frac{3}{2}\theta+\alpha)]\sin\beta$
L_3	$[(1/5)\bar{M}(131-16\bar{M}^2)\cos\theta$ $+ (i/2)(19\bar{M}^2-39/4)\sin\theta]\cos\beta$	$[(1/2)\bar{M}(7\bar{M}^2-67/4)\cos(\frac{3}{2}\theta+\alpha)$ $+ (i/4)(19\bar{M}^2-207/4)\sin(\frac{3}{2}\theta+\alpha)]\sin\beta$

To illustrate the foregoing theory we have used it to calculate the scattering length for Tb^{3+}. Our results for the matrix element (5.1) are obtained from the entries in table 4.

If the axis of the spiral arrangement of the terbium ions lies in the plane of scattering, spanned by the axes x and y, the magnetic moments are in a plane that is parallel to the z-axis, and the intersection with the plane of scattering is at an angle α with respect to the x-axis. For a first-order satellite the Bragg condition selects $\exp(i\beta)$ in $\sin\beta$ and $\cos\beta$, since β is the turn angle for the spiral. Looking at the entries in table 4 it is notable that the terms even and odd in $\bar{M}$ are 90° out of phase, and the cross-sections are even functions of the primary energy. Regarding the dependence of $\langle f\rangle$ on θ, the entries in table 4 can be compared to the findings derived from the idealized scattering length, which means the entries in table 1 for $K = 1$. One notes that the improved picture of the resonant

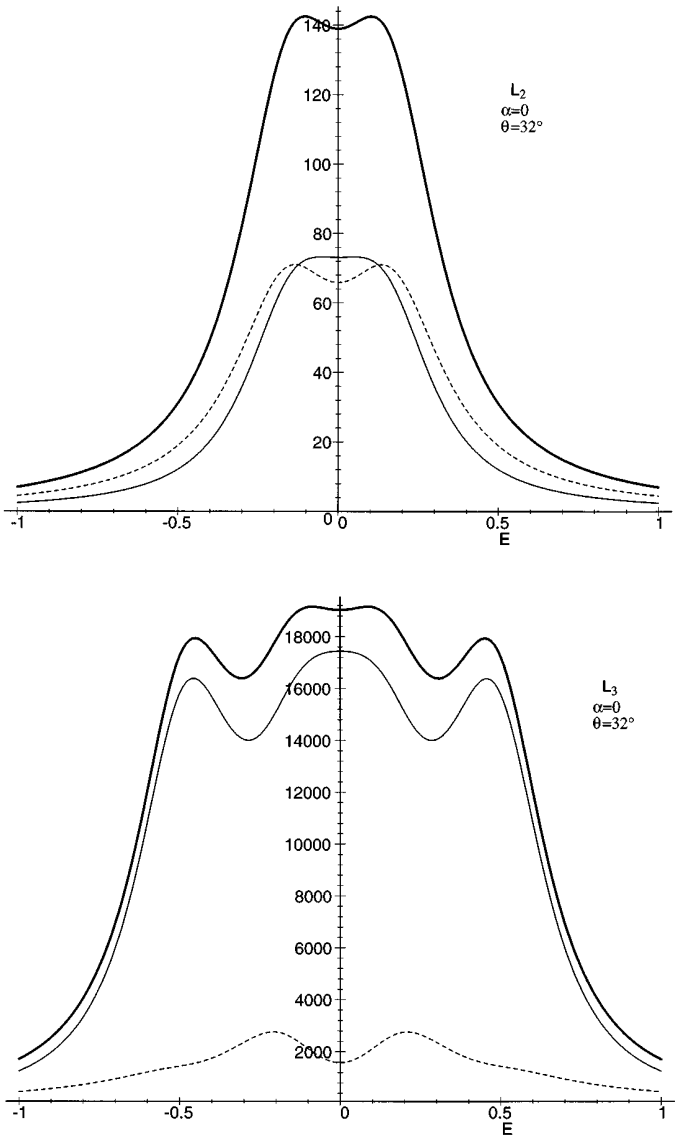

Figure 1. The displayed quantity is $|\langle f\rangle|^2$ where $\langle f\rangle$ is defined in (5.4). The results are appropriate for a first-order satellite from the spiral phase of terbium metal, and the configuration $4f^8$. To obtain the value of the diffraction cross-section multiply the numerical values in a drawing by $((qe)^2\Phi F_J(1)/3528)^2$. The primary energy E is measured relative to an edge in units of Δ_0, and $\gamma = 0.4\Delta_0$. Results for the $\sigma'\sigma$- and $\pi'\sigma$-channels of scattering are, respectively, denoted by a thin solid and a thin dotted line, and the sum of the two channels is given by a thick solid line. At each absorption edge $\alpha = 0$ or $\pi/2$, and for each α the values of θ are 32°, 60° or 66°; the values of the angles are given on each panel. The axis of the spiral lies in the plane of scattering and it is perpendicular (parallel) to the scattering vector, $\boldsymbol{k}$, for $\alpha = 0$ ($\pi/2$). Note that in the calculations θ is constant at an edge, whereas strictly it varies with E so as to satisfy $k = (2E/\hbar c)\sin(\theta/2)$ with $\boldsymbol{k}$ fixed by the position of the Bragg reflection (here a first-order satellite) in reciprocal space. In the present case the variation in θ with E in a panel is expected to be very slight because Δ_0 is very small compared to the energy of an absorption edge, which is of the order of 8 keV.

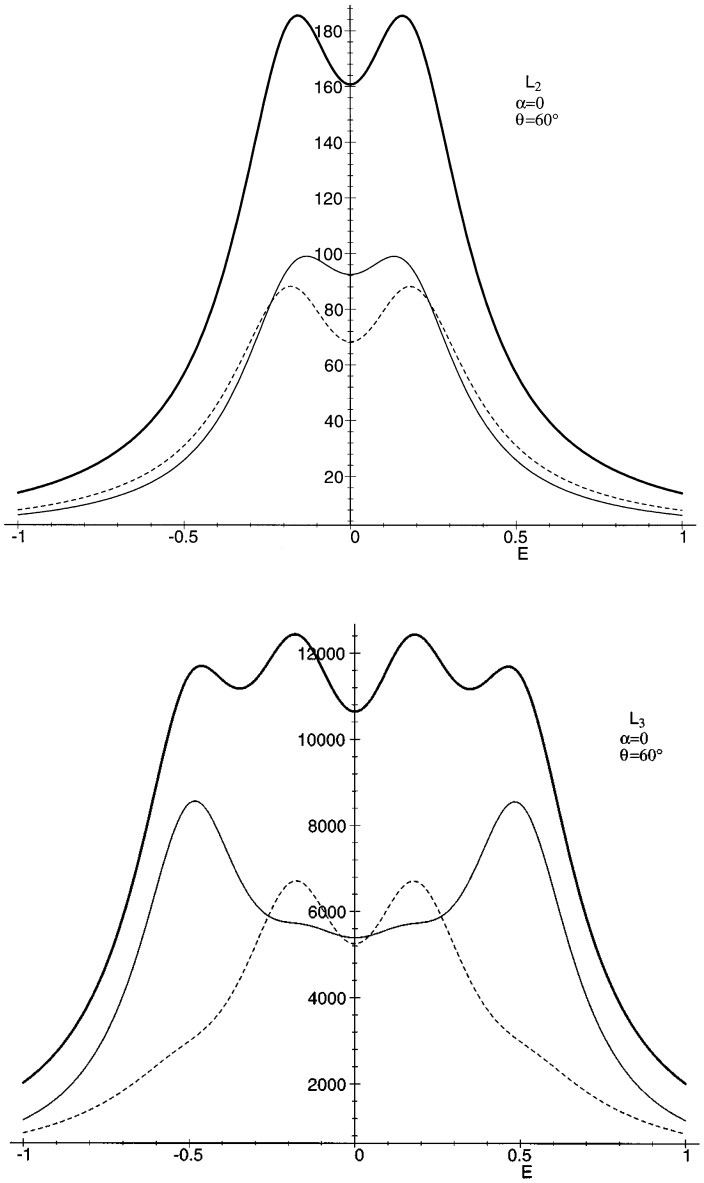

Figure 1. (Continued)

scattering length gives a significantly different dependence on θ to that found with the idealized scattering length.

In figure 1 we display $|\langle f\rangle|^2$ as a function of the primary energy, for various values of θ and α, at the L_2 and L_3 absorption edges. For $\langle f\rangle$ we use

$$\langle f\rangle = -(qe)^2 \sum_{\bar{M}} \frac{\langle Z(\mu;\mu{:}\,\boldsymbol{R}_0)\rangle_\eta}{(E-\Delta(\bar{M})+(\mathrm{i}/2)\gamma)} \tag{5.4}$$

with $\langle Z\rangle_\eta$ constructed from the entries in table 4. These are evaluated with $\cos\beta \to 1/2$

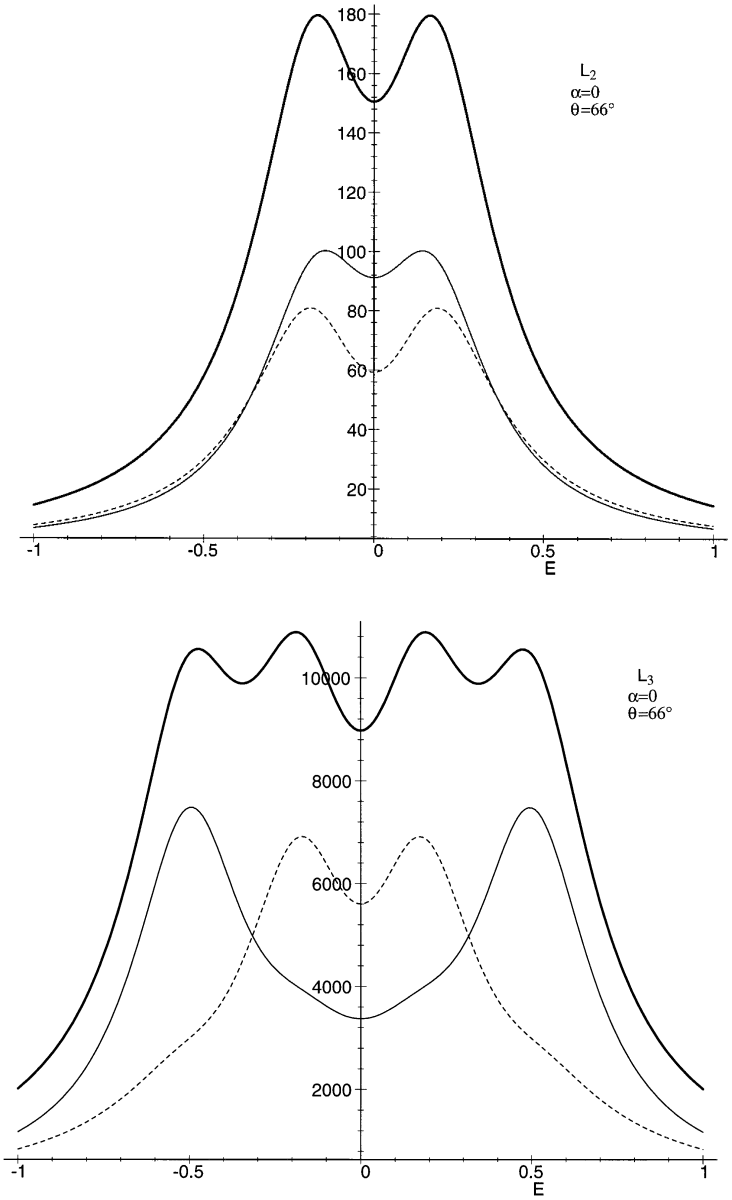

Figure 1. (Continued)

and $\sin\beta \to -\mathrm{i}/2$, which are appropriate for a first-order satellite reflection. Thus, at each absorption edge, $|\langle f\rangle|^2$ is the coherent sum of $2\bar{J}+1$ oscillators. For γ we have chosen a constant value, independent of both $\bar{M}$ and $\bar{J}$.

Looking at the panels in figure 1, perhaps the first thing that comes to one's attention is that the maximum intensities at the L_2 and L_3 edges differ by a factor of about 100. This factor is in line with the prediction from table 3, based on the idealized scattering length, since the entry for $K = 1$ differs by 10 at the L_2 and L_3 edges. Other factors which enter

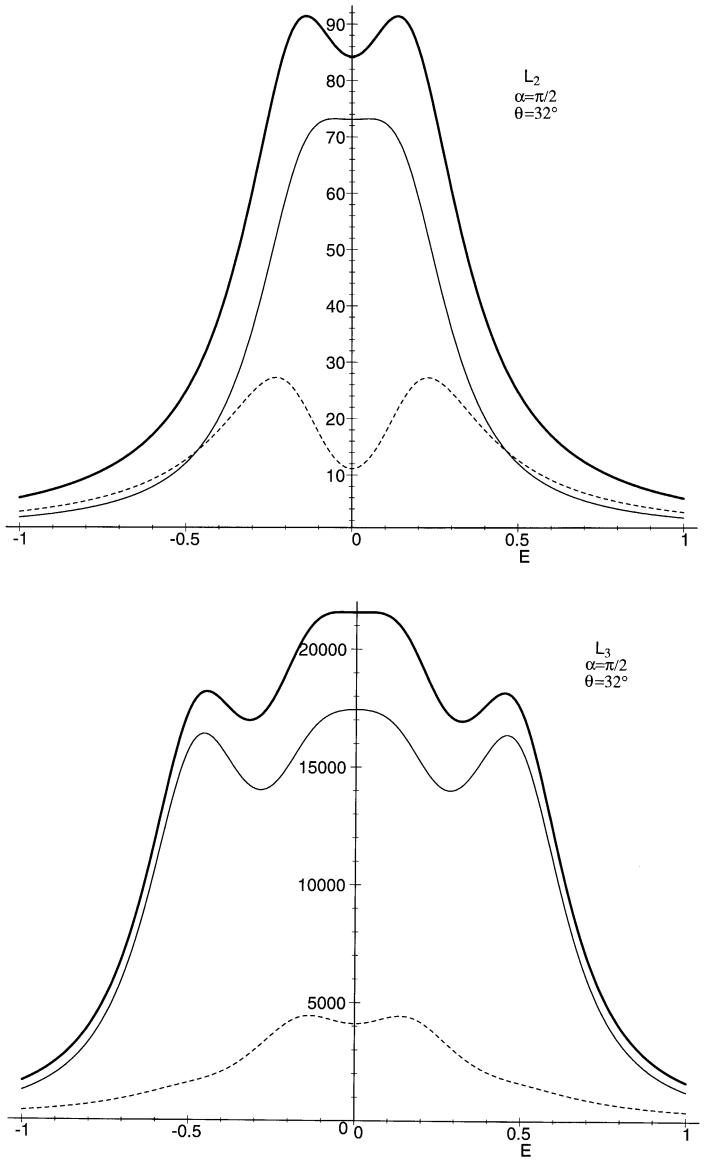

Figure 1. (Continued)

the relative intensity at the two edges, and are not taken into account in this observation, are that the E2 cross-section scales with E^8 and γ might depend on $\bar{J}$.

Using the idealized scattering length as a point of reference for the intensity, one anticipates that in the $\pi'\sigma$-channel the intensity depends on α while in the $\sigma'\sigma$-channel it is independent of α. The panels in figure 1 do indeed show this trend with α; for $\alpha = \pi/2$ the $\sigma'\sigma$-channel dominates and, for $\alpha = 0$, the intensities in the two channels are similar in size, except at the L_3 edge and for $\theta = 32^\circ$. At the L_3 edge there are significant changes in the shapes of the lines as a function of θ and they are most pronounced in the $\sigma'\sigma$-channel. The total intensity at the L_3 edge decreases with increasing θ, by as much as

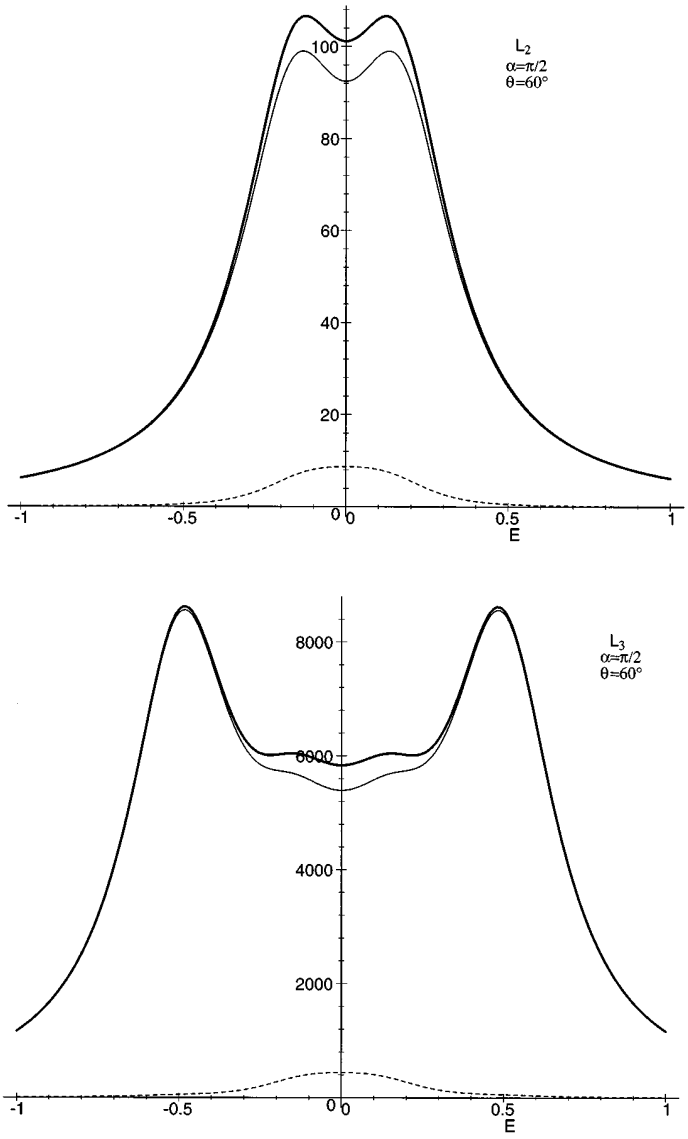

Figure 1. (Continued)

almost a factor of three for $\alpha = \pi/2$, and at the L_2 edge the fractional change with θ is much smaller and in the opposite direction.

6. Polarization effects

A primary beam from a synchrotron source of x-rays is adequately described by a Stokes vector with two parameters, and following Lovesey and Collins (1996) we find $\boldsymbol{P} = (0, P_2, P_3)$ with $P_2^2 + P_3^2 \leqslant 1$. The equality is achieved for a beam with complete polarization. In previous sections we have considered pure σ-polarization which is described

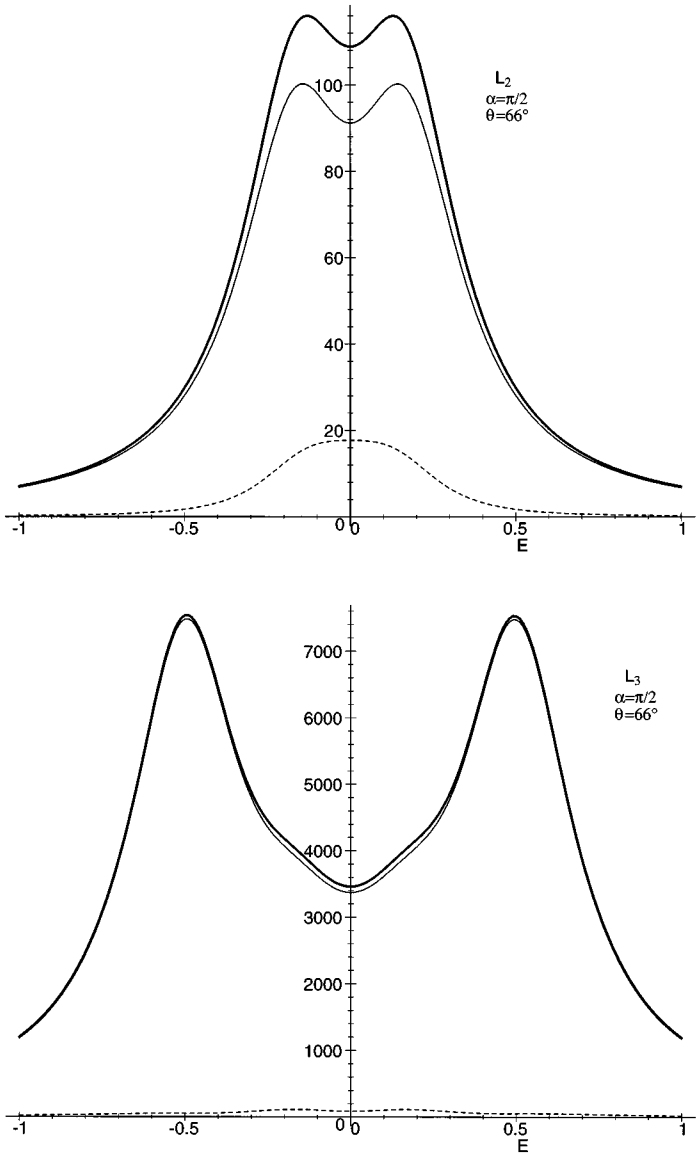

Figure 1. (Continued)

by $P_2 = 0$ and $P_3 = +1$. The parameter P_2 is the mean helicity in the beam.

Let us label the four scattering lengths following the scheme used in table 1, which is $\varepsilon'\varepsilon$ for primary and secondary polarization ε and ε', respectively. The corresponding scattering length we denote simply by $(\varepsilon'\varepsilon)$, i.e. $(\varepsilon'\varepsilon) \equiv \langle f \rangle^{(\varepsilon'\varepsilon)}$. With this convention the cross-section is

$$|\langle f \rangle|^2 = P_2 \,\mathrm{Im}\{(\sigma'\sigma)(\sigma'\pi)^* + (\pi'\sigma)(\pi'\pi)^*\} + \frac{1}{2}(1+P_3)\{|(\sigma'\sigma)|^2 + |(\pi'\sigma)|^2\}$$
$$+ \frac{1}{2}(1-P_3)\{|(\pi'\pi)|^2 + |(\sigma'\pi)|^2\}. \tag{6.1}$$

At a synchrotron source a standard setting is $P_2 = 0$ and $P_3 \sim 1.0$.

As an illustration of the cross-section (6.1) we evaluate it for the model of a lanthanide ion (4.1). The arrangement of the ions is described in the preceding section, and we again treat the intensity of the first-order satellite using the tensor of rank one, which should describe to a good approximation the properties at a high temperature. In the following result, the coefficient of $(1 + P_3)/2$ is taken from table 1. The remaining components are readily derived using results given by Lovesey (1996). In making the calculations it is helpful to use the identity

$$\{H^K_{m_0}\}^{\pi'\sigma} = (-1)^K(\{H^K_{m_0}\}^{\sigma'\pi})^*.$$

The cross-section for the first-order satellite is the product of

$$\frac{\{\frac{1}{40}(qe)^2\Phi\Psi_\mu(1)\}^2}{\{(E-\Delta)^2 + (\frac{1}{2}\Gamma)^2\}_{\bar{J}}}$$

and the following geometric factor:

$$\pm P_2 \sin\theta\left\{\sin\left(\alpha - \frac{3\theta}{2}\right) + 4\cos\theta\sin\left(\alpha + \frac{3\theta}{2}\right)\right\} + \frac{1}{2}(1+P_3)\left\{\sin^2\theta + \sin^2\left(\alpha + \frac{3\theta}{2}\right)\right\}$$
$$+ \frac{1}{2}(1-P_3)\{4\sin^2 2\theta + \sin^2\left(\alpha - \frac{3\theta}{2}\right)\}. \qquad (6.2)$$

A few comments are in order about the first term, proportional to the mean helicity in the beam. The sign goes with $\boldsymbol{k} \pm \boldsymbol{Q} = \boldsymbol{\tau}$ where $\boldsymbol{Q}$ is the wave vector of the spiral (turn angle $\beta = \boldsymbol{Q}\cdot\boldsymbol{R}_0$) and $\boldsymbol{\tau}$ is a reciprocal-lattice vector. It is interesting to observe that the term in P_2 can vanish, e.g. $\theta = 60^\circ$ and $\alpha = \pi/2$, and it is not symmetrical with respect to α and $-\alpha$. Addressing the other two terms in (6.2), note that the coefficient of $1 - P_3$ can be much larger than the coefficient of $1 + P_3$. Consider the axis of the spiral aligned with $\boldsymbol{k}$ ($\alpha = \pi/2$) and a scattering angle $\theta = 60^\circ$. For this setting the ratio of the factors is 4, and taking $P_3 = 0.90$ the third term in the cross-section is as much as 21% of the second term.

The cross-section for a first-order satellite that we have derived is proportional to the square of the magnetic moment, due to the presence in the cross-section of the factor $\Psi^2_\mu(1)$. For the same set of basic assumptions, a different dependence of the cross-section on temperature is found if the Bragg reflection is indexed by the chemical unit cell. This effect is present in our discussion of diffraction by gadolinium. To illustrate it in a different context we will now calculate the cross-section proportional to P_2, for a Bragg reflection from a ferromagnetic arrangement of the ions. We limit the calculation to the lowest-order tensors, and at an elevated temperature they certainly give the dominant contribution to the cross-section.

An inspection of the products in the contribution proportional to P_2 reveals that in the double sum, in which a term is the product of two tensors with ranks K and K', the non-zero parts of the sum have $K + K' =$ odd integer. (A term in the double sum with $K + K' =$ even is purely real.) A straightforward calculation leads to the result

$$P_2\,\mathrm{Im}\{(\sigma'\sigma)(\sigma'\pi)^* + (\pi'\sigma)(\pi'\pi)^*\} = -\frac{1}{2}P_2\frac{(\frac{1}{10}(qe)^2\Phi)^2\Psi_\mu(0)\Psi_\mu(1)}{((E-\Delta)^2 + (\frac{1}{2}\Gamma)^2)_{\bar{J}}}$$
$$\times\ \sin\beta\left\{\cos\theta\sin\left(\alpha - \frac{3\theta}{2}\right) + \cos 2\theta\sin\left(\alpha + \frac{3\theta}{2}\right)\right\}. \qquad (6.3)$$

Several features of this result deserve comment. First, the result is proportional to $\sin\beta$ and it therefore vanishes if the magnetic moment is perpendicular to the plane of scattering.

Secondly, the other trigonometric factor is zero for certain θ and α, e.g. $\theta = 60^\circ$ and $\alpha = \pi/2$, and $\theta = 120^\circ$ and $\alpha = 0$. Lastly, the result is proportional to the magnetic moment. This feature is in keeping with physical intuition, scilicet, in the cross-section there is a product of the two axial vectors in the problem (helicity and the magnetic moment). Set against this, there is something of a need to comment on the preceding result (6.2) for a first-order satellite in which P_2 is multiplied by the square of the magnetic moment.

In this regard, the essential features in the physics behind the result (6.2) is that for a satellite reflection the Bragg condition selects components from $\cos n\beta$ and $\sin n\beta$ and these are out of phase by 90°. The outcome is that the diagonal and off-diagonal channels of scattering are out of phase by 90°, and so even for $K = K' = 1$ the coefficient of P_2 is not zero. By contrast, in (6.3) for a ferromagnetic reflection all channels have purely real or purely imaginary amplitudes according to whether the rank is even or odd. As we have previously noted, the non-zero parts in the coefficient of P_2 are products of tensors whose ranks satisfy $K + K' =$ odd integer. At the level of approximation to which we are working, the coefficients of $1 \pm P_3$ do not depend on the magnetic state of the resonant ion.

In our discussion of the polarization of the secondary beam we start with the linear polarization which is described by parameter P_3'. Using again results from Lovesey and Collins (1996), and setting $\boldsymbol{P} = (0, 0, P_3)$, we find

$$P_3' = \{(1 + P_3)[|(\sigma'\sigma)|^2 - |(\pi'\sigma)|^2] + (1 - P_3)[|(\sigma'\pi)|^2 - |(\pi'\pi)|^2]\}/(2|\langle f\rangle|^2). \tag{6.4}$$

Here, the denominator is obtained from (6.1) with $P_2 = 0$.

We evaluate (6.4) for a first-order satellite from a spiral arrangement of the ions, with the axis of the spiral parallel to the plane of scattering. As in the preceding treatment of this model, we limit the discussion to the lowest-rank tensor. The result is

$$P_3' = -\left\{(1 + P_3)\sin\left(\alpha + \frac{\theta}{2}\right)\sin\left(\alpha + \frac{5\theta}{2}\right) + (1 - P_3)\left[4\sin^2 2\theta - \sin^2\left(\alpha - \frac{3\theta}{2}\right)\right]\right\}\Big/(2 \times \text{equation (6.2)}) \tag{6.5}$$

where the denominator is twice the value of (6.2) with $P_2 = 0$. Note that (6.5) holds for the L_2 and L_3 absorption edges. If we include in the evaluation of (6.4) the rank-three tensor, P_3' can be different at the two edges because, in this case, the numerator and the denominator are linear combinations of $\Psi_\mu^2(1)$ and $\Psi_\mu^2(3)$. By the same argument, when $\Psi_\mu^2(3)$ is included in the evaluation of (6.4), P_3' will depend on the temperature. However, as we have stressed, at an elevated temperature $\Psi_\mu^2(1) \gg \Psi_\mu^2(3)$.

The result (6.5) with $P_3 = 0.9$ is displayed in figure 2 (dashed curve). It is shown as a function of θ, the angle through which the x-ray beam is deflected, for $\alpha = \pi/2$. Results for $\alpha = 0$ are obtained simply by inverting the graph in figure 2 about the value $\theta = 90^\circ$. For $\alpha = \pi/2$ one finds, at $\theta = 0^\circ$, the secondary polarization $P_3' = -P_3$, and with the opposite extreme value, $\theta = 180^\circ$, it has the value $P_3' = -5(6 - 5P_3)/(43 - 30P_3)$. For $\alpha = \pi/4$ one finds that P_3' is symmetric about $\theta = 90^\circ$, where $P_3' = 1$, and for $\theta = 0^\circ$ and 180°, $P_3' = -P_3$. The variation of P_3' with θ is pronounced and this should be easy to monitor in an appropriate experiment.

For a primary beam with $\boldsymbol{P} = (0, 0, P_3)$ the mean helicity in the secondary beam is

$$P_2' = \mp\mathrm{Im}\{(1 + P_3)(\sigma'\sigma)(\pi'\sigma)^* + (1 - P_3)(\sigma'\pi)(\pi'\pi)^*\}/|\langle f\rangle|^2 \tag{6.6}$$

with $|\langle f\rangle|^2$ obtained from (6.1). As there is no circular polarization in the primary beam ($P_2 = 0$), equation (6.6) gives the circular polarization created in the scattering event recorded at the setting $\boldsymbol{k} \pm \boldsymbol{Q} = \boldsymbol{\tau}$.

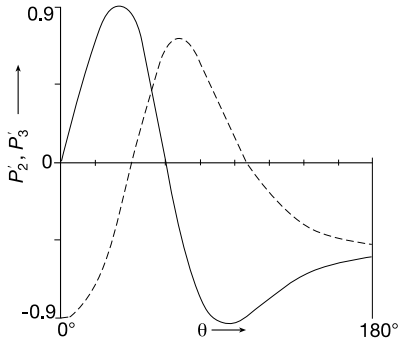

Figure 2. States of polarization in the secondary beam, described by the parameters P_2' and P_3', are displayed as a function of θ for a first-order satellite, for which $\boldsymbol{Q}+\boldsymbol{k}=\boldsymbol{\tau}$, and $P_3=0.9$ and $\alpha=\pi/2$. The values shown in the graph are for P_3' (dashed curve) obtained from (6.5) and P_2' (solid curve) obtained from (6.7) taken with the positive sign. For the chosen value of α, the axis of the spiral arrangement of the ions is aligned with $\boldsymbol{k}$.

Evaluated for our model of a first-order satellite, equation (6.6) for P_2' can be different from zero because the diagonal and the off-diagonal scattering lengths differ in phase by 90°. We find

$$P_2' = \pm\sin\theta\left\{(1+P_3)\sin\left(\alpha+\frac{3\theta}{2}\right)+4(1-P_3)\cos\theta\sin\left(\alpha-\frac{3\theta}{2}\right)\right\}\Big/\text{equation (6.2)} \tag{6.7}$$

where, as in the companion expression for P_3', the denominator is the value of (6.2) for $P_2=0$. Evaluated for $\alpha=\pi/2$, so that the axis of the spiral is aligned with the scattering vector,

$$P_2' = 0 \qquad \theta = 0^\circ$$

and

$$P_2' = \mp 6(5P_3-3)/(43-30P_3) \qquad \theta = 180^\circ.$$

Figure 2 contains P_2' for $\alpha=\pi/2$, $P_3=0.9$ and $\boldsymbol{k}+\boldsymbol{Q}=\boldsymbol{\tau}$ as a function of θ. To obtain a value of P_2' for $\alpha=0$ from the results in figure 2, invert the graph about 90° and change the sign of the displayed value. It is interesting to find that P_2' is a strong signature of the scattering, attaining values in the range $-0.93 \leqslant P_2' \leqslant 0.89$ for $P_3=0.9$. Our remarks about P_3' concerning its dependence on $\bar{J}$ and the temperature also apply to P_2'.

7. Summary

We have calculated the E2 (electric quadrupole) contribution to the scattering length using an atomic model for the resonant ion. The atomic model is expected to be more than reasonable for lanthanide ions.

With an idealized form for the scattering length, in which an absorption edge is uniquely specified by the total angular momentum of the core state that accepts a hole from the valence shell, our most general expression for the Bragg scattering length is obtained by combining (2.1), and (3.1) and (3.5). The atomic matrix element in the scattering length depends on the properties of the valence shell, of course. These properties can be expressed in terms of matrix elements of various atomic operators, constructed with the spin and orbital angular

momentum operators of the valence holes, and examples of the expressions are found in (4.10)–(4.12). Sum rules, often used to analyse data, on the dichroic signal in the attenuation coefficient are contained within the idealized scattering length.

By way of an orientation to the theory described in the foregoing paragraph we have evaluated it for a simple and realistic description of a lanthanide ion. The simplification made is to take the atomic matrix element as diagonal with respect to the magnetic quantum numbers. For this special case, in (3.5) the element of the rotation matrix reduces to a spherical harmonic. The angular dependence of the scattering length is then easy to evaluate, and our results are listed in table 1. The thermodynamic and atomic properties of the valence shell are the subjects of tables 2 and 3. The atomic properties in table 3 are for the ground state specified by Hund's rules, and for lanthanide ions this is expected to be a good approximation. The entries in table 1 describe in full the case of a complete polarization in the primary beam which is perpendicular to the plane of scattering. In section 6 we provide the cross-section, and an illustrative example for a first-order satellite, appropriate when the primary beam contains circular polarization, and less-than-complete linear polarization. Also considered is the polarization in the secondary beam.

If the wave function for the valence shell is not diagonal with respect to the magnetic quantum numbers the complete form of the atomic matrix element is needed, and in this case (3.10) is the required expression. One can readily incorporate a knowledge of the valence shell better than the specification by Hund's rules simply by entering the superior estimates in (4.10)–(4.12). Alternatively, one can use (3.5) and the expansion of the atomic matrix element in terms of Racah unit tensors (Lovesey and Balcar 1997a).

Core-level structure in the scattering length can be introduced by using an expression for the scattering length derived by Lovesey (1997). In this paper, its use is illustrated in a discussion of diffraction at the first-order satellite from the spiral arrangement of ions in terbium metal. The prediction is that at the L_3 edge the diffraction signal as a function of energy can be highly structured, and the structure changes with the setting of the spiral relative to the geometry of the primary and secondary beams. On the other hand, the shape of the line at the L_2 edge, when compared to that at the L_3 edge, is almost without structure.

Previous work by Hill and McMorrow (1996) on the theory of Bragg diffraction enhanced by an E2 absorption event focuses on the geometric features of the diffraction signal, and they mention attempts at the calculation of the atomic matrix element. In the language for an E2 event used in this paper, which follows Lovesey (1996), their main results are values for the spherical tensor $\mathbf{H}^{(K)}$, and for a diagonal atomic matrix element their findings condense to the entries in table 1.

Acknowledgment

We have benefited from discussions with Dr S P Collins.

Note added in proof. Two pertinent pieces of work are reported by Matsuyama *et al* (1997) and Bartolomé *et al* (1997).

References

Bartolomé F, Tonnerre J M, Sève L, Raoux D, Chaboy J, García L M, Krisch M and Kao C C 1997 *Phys. Rev. Lett.* **79** 3775

Carra P 1997 private communication

Detlefs C, Islam A H M Z, Goldman A I, Stassis C, Canfield P C, Hill J P and Gibbs D 1997 *Phys. Rev.* B **55** R680
Gibbs D, Harshman D R, Isaacs E D, McWhan D B, Mills D and Vettier C 1988 *Phys. Rev. Lett.* **61** 1241
Giorgetti C, Dartyge E, Brouder Ch, Baudelet F, Meyer C, Pizzini S, Fontaine A and Galéra R-M 1995 *Phys. Rev. Lett.* **75** 3186
Hannon J P, Trammell G T, Blume M and Gibbs D 1988 *Phys. Rev. Lett.* **61** 1245 (erratum 1989 **62** 2644)
Hill J P and McMorrow D F 1996 *Acta. Crystallogr.* A **52** 236
Jensen J and Mackintosh A R 1991 *Rare Earth Magnetism: Structures and Excitations* (Oxford: Clarendon)
Judd B R 1975 *Angular Momentum Theory for Diatomic Molecules* (New York: Academic)
Lovesey S W 1986 *Condensed Matter Physics: Dynamic Correlations* (Menlo Park, CA: Benjamin/Cummings)
——1996 *J. Phys.: Condens. Matter* **8** 11 009
——1997 *J. Phys.: Condens. Matter* **9** 7501
Lovesey S W and Balcar E 1997a *J. Phys.: Condens Matter* **9** 4237
——1997b *J. Phys.: Condens Matter* **9** 8679
Lovesey S W and Collins S P 1996 *X-ray Scattering and Absorption by Magnetic Materials* (Oxford: Clarendon)
Matsuyama H, Harada I and Kotani A 1997 *J. Phys. Soc. Japan* **66** 337
Namikawa K, Ando M, Nakajima T and Kawata H 1985 *J. Phys. Soc. Japan* **54** 4099
Teramura Y, Tanaka A, Thole B T and Jo T 1996 *J. Phys. Soc. Japan* **65** 3056
van Veenendaal M, Goedkoop J B and Thole B T 1997 *Phys. Rev. Lett.* **78** 1162